

Active Vibration Control of a Smart Beam by Using a Spatial Approach

Ömer Faruk KIRCALI^{1,2}, Yavuz YAMAN²,
Volkan NALBANTOĞLU² and Melin ŞAHİN²

¹*STM Savunma Teknolojileri Muhendislik ve Ticaret A.S., Ankara, TURKIYE*

²*Department of Aerospace Engineering, Middle East Technical University, Ankara,
TURKIYE*

1. Introduction

The vibration control is an important and rapidly developing field for lightweight flexible aerospace structures. Those structures may be damaged or become ineffective under the undesired vibrational loads they constantly experience. Hence, they require effective control mechanism to attenuate the vibration levels in order to preserve the structural integrity. The usage of smart materials, as actuators and/or sensors, has become promising research and application area that gives the opportunity to accomplish the reduction of vibration of flexible structures and proves to be an effective active control mechanism.

For the last few decades there has been an extensive research about the piezoelectric materials because of the capability of being used both as actuators and sensors. The smart structure is a structure that can sense external disturbance and respond to that in real time to fulfil operational requirements. Smart structures consist of passive structure, highly distributed active devices called smart materials/elements and processor networks. The smart materials are primarily used as sensors and/or actuators and are either embedded or attached to an existing passive structure (Çalışkan, 2002). Today, the main and maybe the most widespread application area of piezoelectric materials is using them as collocated actuator and sensor pair for active vibration control purposes (Prasad, 1998).

Active vibration control of a smart structure starts with an accurate mathematical model of the structure. Modeling smart structures may require the modeling of both passive structure and the active parts. Crawley and de Luis (1989), by neglecting the mass of active elements, presented an analytical modeling technique to show that the piezoelectric actuators can be used to suppress some modes of vibration of a cantilevered beam. Similar approach was carried out on thin plates by Dimitridis et al (1991). Although neglecting the mass and stiffness properties of the smart materials compared to the passive structure is generally acceptable, the modeling of a smart structure mainly involves the force and moment descriptions generated by the smart materials. Sample modeling studies are proposed by

several researchers such as Pota et al. (1992), Halim (2002b) The governing differential equations of motion of the smart structures can then be solved by analytical methods, such as modal analysis, assumed-modes method, Galerkin's method or finite element method (Meirovitch, 1986).

Since it is not so easy to consider all non-uniformities in structural properties of a smart structure, the analytical modeling techniques such as finite element model, modal analysis or assumed modes method allow one to obtain system model including only the approximate information of optimal placement of piezoelectric patches, natural frequencies and mode shapes of the structure except damping (Çalışkan, 2002 and Halim, 2002b). In order to improve the model, Nalbantoğlu (1998) and Nalbantoğlu et al. (2003) showed that experimental system identification techniques can be applied on flexible structures and they may help one to identify the system more accurately.

Due to having a large number of resonant modes, the high frequency characteristics of a flexible structure generally cause problems in identifying the system method. Since, usually the first few vibrational modes are taken into account in the controller design, the reduction of the model is often required to obtain the finite-dimensional system model (Hughes, 1981; Balas, 1995 and Moheimani, 1997). General approach for reducing the order of the model is the direct model reduction. However, removing the higher modes directly from the system model perturbs zeros of the system (Clark, 1997). Minimizing the effect of model reduction and correcting the system model is possible by adding a feedthrough, or correction, term including some of the removed modes, to the truncated model (Clark, 1997; Moheimani, 2000d and Moheimani, 2000c). Halim (2002b) proposed an optimal expression for feedthrough term in case of undamped and damped system models.

Various control techniques have been used as active control strategy like optimal control (Hanagoud, 1992), LQG control (Bai, 1996) and robust control using H_∞ (Nalbantoğlu, 1998; Yaman, 2001 and Ülker, 2003) or H_2 control framework (Halim, 2002c). The H_∞ control design technique for robust control phenomena has been developed by many researchers for various application areas including the vibration control (Zames, 1981; Francis, 1984; Doyle, 1989 and Lenz, 1993). Yaman et al. (2001, 2003b) showed the effect of H_∞ based controller on suppressing the vibrations of a smart beam due its first two flexural modes. They also extended their studies to a smart plate (2002a, 2002b). Ülker (2003) showed that, besides the H_∞ control technique, μ -synthesis based controllers can also be used to suppress vibrations of smart structures. In all those works on flexible structures, the general control strategy focused on analyzing the vibrations at specific locations over the structure and minimizing them. However, that kind of pointwise controller design ignores the effect of vibration at the rest of the body and a successful vibration reduction over entire structure can not always be accounted for.

Moheimani and Fu (1998c) introduced spatial H_2 norm, which is a measured performance over spatial domain, for spatially distributed systems in order to meet the need of spatial vibration control. Besides, Moheimani et al. (1997, 1998a) proposed spatial H_∞ norm

concept and simulation based results of spatial vibration control of a cantilevered beam were presented. Moheimani et al. (1998b, 1999) carried out the spatial approach on feedforward and feedback controller design, and presented illustrative results. They also showed that spatial H_∞ controllers could be obtained from standard H_∞ controller design techniques. Although the simulations demonstrated successful results on minimizing the vibrations over entire beam, implementation of that kind of controllers was not guaranteed on real world systems. Halim (2002b, 2002c) studied the implementation of spatial H_2 controllers on active vibration control of a simply-supported beam experimentally and presented successful results. He continued to work on simply-supported beams about implementation of spatial H_∞ controller and obtained successful experimental results (Halim, 2002a). Further experimental studies were performed on active vibration control of a simply-supported piezoelectric laminate plate by Lee (2005). Lee also attenuated acoustic noise due to structural vibration.

The current chapter aims to summarize the studies of modelling and spatial control of a cantilevered beam (Kircalı et al. 2008, 2007, 2006a and 2006b).

2. Assumed-Modes Modeling of the Smart Beam

Consider the cantilevered smart beam model used in the study which is depicted in Fig.1. The smart beam consists of a passive aluminum beam (507mmx51mmx2mm) with eight symmetrically surface bonded SensorTech BM500 type PZT (Lead-Zirconate-Titanate) patches (25mmx20mmx0.5mm), which are used as the actuators. Note that, in this study, the group of PZT patches on one side of the beam is considered as if it is a single patch. The beginning and end locations of the PZT patches along the length of the beam away from the fixed end are denoted as r_1 and r_2 , and the patches are assumed to be optimally placed (Çalışkan, 2002). The subscripts b , p and sb indicate the passive beam, PZT patches and smart beam respectively. Analytical modeling of the smart beam is performed by assumed-modes method, which represents the deflection of the beam by means of a series solution:

$$y(r, t) = \sum_{i=1}^N \phi_i(r) q_i(t) \quad (1)$$

where ϕ_i are admissible functions which satisfy the geometric boundary conditions of the passive beam, q_i are time-dependent generalized coordinates, r is the longitudinal axis and t is time. Assumed-modes method uses this solution to obtain approximate system model of the structure with the help of energy expressions (Mason, 1981). The kinetic and potential energies of the smart beam can be determined to be (Kircalı, 2006a):

$$T_{sb}(t) = \frac{1}{2} \sum_{i=1}^N \sum_{j=1}^N \left\{ \int_0^{L_b} \rho_b A_b \phi_i \phi_j dr + 2 \int_{r_1}^{r_2} \rho_p A_p \phi_i \phi_j dr \right\} \dot{q}_i \dot{q}_j \quad (2)$$

$$V_{sb}(t) = \frac{1}{2} \sum_{i=1}^N \sum_{j=1}^N \left\{ \int_0^{L_b} E_b I_b \phi_i'' \phi_j'' dr + 2 \int_{r_1}^{r_2} E_p I_p \phi_i'' \phi_j'' dr \right\} q_i q_j \quad (3)$$

The total viscous damping force of the smart beam can similarly be obtained as (Kircali, 2006a):

$$F_{sb} = \frac{1}{2} \sum_{i=1}^N \sum_{j=1}^N \left\{ \int_0^{L_b} (2\xi_i \omega_i) \rho_b A_b \phi_i \phi_j dr + 2 \int_{r_1}^{r_2} (2\xi_i \omega_i) \rho_p A_p \phi_i \phi_j dr \right\} \dot{q}_i \dot{q}_j \quad (4)$$

where the beam’s density, Young’s modulus of elasticity, second moment of area and cross sectional area are defined as ρ_b , E_b , I_b , and A_b respectively. Also note that subscript i and j yield number of eigenvalues, ξ_i is the viscous damping coefficient of the i^{th} mode and ω_i represents the i^{th} natural frequency of the beam.

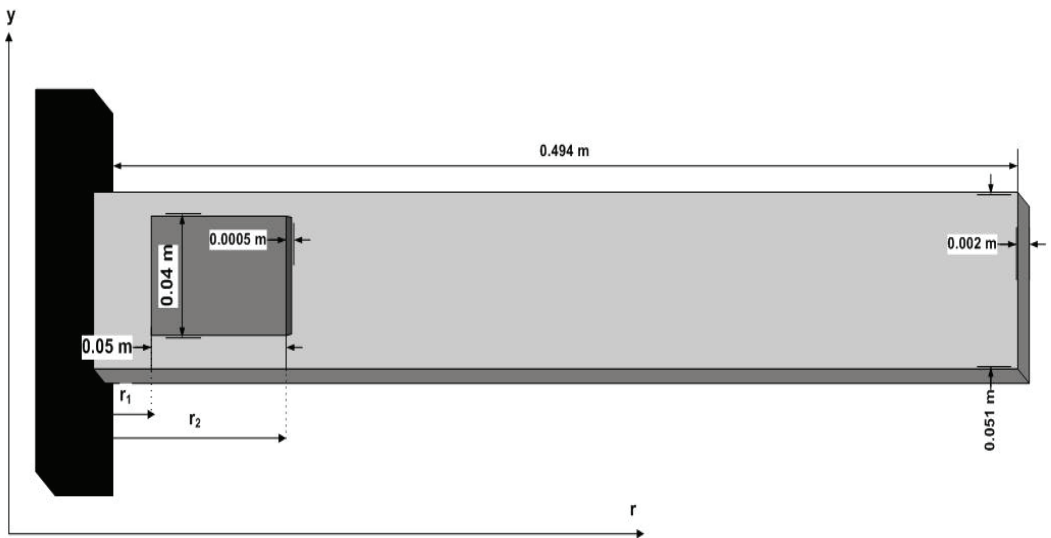


Fig. 1. The smart beam model used in the study

The PZT patches are placed in a collocated manner and the voltage is applied in order to create a bimorph configuration (PZT patches bonded to opposite faces of the beam have opposite polarity), the resulting effect on the beam becomes equivalent to that of a bending moment. This case is shown in Fig.2:

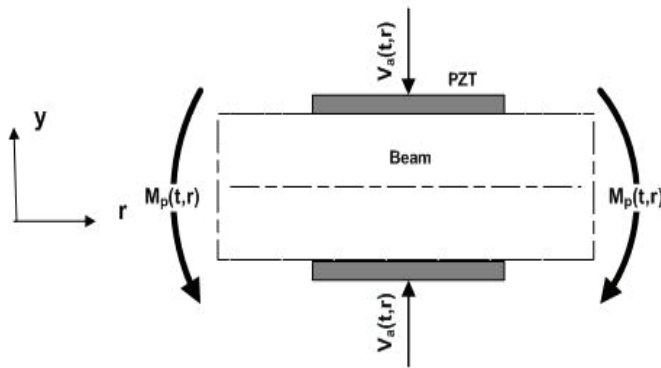


Fig. 2. Inducing bending moment by applying voltage to PZT patches

Here $M_p(t, r)$ denotes the bending moment and $V_a(t, r)$ is the applied voltage. When the voltage is applied on a PZT patch, a piezoelectric strain ε_p is introduced in the patch (Baz, 1988):

$$\varepsilon_p(t, r) = \frac{d_{31}}{t_p} V_a(t, r) \quad (5)$$

The longitudinal stress consequently generates a bending moment about the neutral axis of the system, as:

$$M_p(t, r) = C_p V_a(t, r) \quad (6)$$

where C_p is a geometric constant due to bending moment, and expressed as:

$$C_p = E_p d_{31} w_p (t_p + t_b) \quad (7)$$

As a consequence, the transfer function, $G_N(s, r)$, from the input voltage to the beam deflection in the frequency domain, including N number of eigenfunctions, is obtained as:

$$G_N(s, r) = \sum_{i=1}^N \frac{\bar{P}_i \phi_i(r)}{s^2 + 2\xi_i \omega_i s + \omega_i^2} \quad (8)$$

where

$$\bar{P}_i = \frac{C_p [\phi'_i(r_2) - \phi'_i(r_1)]}{\{\rho AL^3\}_{sb}} \quad (9)$$

and

$$\{\rho AL^3\}_{sb} = \rho_b A_b L_b^3 + 2\rho_p A_p L_p^3 \quad (10)$$

The detailed derivation of equation (8) can be found in (Kırcalı, 2006a). In this study, the assumed modes (i.e. the admissible functions) of the fixed-free smart beam are taken as the eigenfunctions of the fixed-free passive beam:

$$\phi_i(r) = L_b \left\{ \cosh \beta_i r - \cos \beta_i r - \frac{\cos \beta_i L_b + \cosh \beta_i L_b}{\sin \beta_i L_b + \sinh \beta_i L_b} (\sinh \beta_i r - \sin \beta_i r) \right\} \quad (11)$$

3. Model Correction and Spatial Identification of the Smart Beam

Assumed-modes method uses admissible functions in order to model the dynamics of the system, but ignores the nonuniform mass and stiffness distributions. If one uses a large number of admissible functions, or more general if their number goes to infinity, the model will be exactly the same as the original one. However, using infinite number of admissible functions is not convenient to apply for real structures at least for huge amount of computing requirements. Therefore, it is generally believed that the utilization of sufficiently large number of admissible functions will be enough to increase the accuracy of the approximate system model (Hughes, 1987).

Including large number of admissible functions leads to not only a more accurate but also a high order approximate system model. Since the order of an H_∞ controller depends on the system order, such a higher order model yields an excessive order controller which may not be possibly implemented. However, the controller design techniques generally focus on a particular bandwidth which includes only a few vibration modes of the system. In this respect, the reduction of the order of the model is required.

One of the most popular techniques for reducing the order of the system model is the direct model reduction, which simplifies the system model by directly truncating the higher modes of frequency range of interest. However, removing the higher modes may perturb the zeros of the system which will affect the closed-loop performance and stability (Clark, 1997). One particular approach to compensate the error of the model truncation was

presented by Moheimani (Moheimani, 2000a) which considers adding a correction term that minimizes the weighted spatial H_2 norm of the truncation error. The additional correction term had a good improvement on low frequency dynamics of the truncated model. Moheimani (2000d) and Moheimani et al. (2000c) developed their corresponding approach to the spatial models which are obtained by different analytical methods. Moheimani (2006b) presented an application of the model correction technique on a simply-supported piezoelectric laminate beam experimentally. However, in all those studies, the damping in the system was neglected. Halim (2002b) improved the model correction approach with damping effect in the system. This section will give a brief explanation of the model correction technique with damping effect based on those previous works (Moheimani, 2000a, 2000c and 2000d) and for more detailed explanation the reader is advised to refer to the reference (Moheimani, 2003).

Recall the transfer function of the system from system input to the beam deflection including N number of modes given in equation (8). The spatial system model expression includes N number of resonant modes assuming that N is sufficiently large. The controller design however interests in the first few vibration modes of the system, say M number of lowest modes. So the truncated model including first M number of modes can be expressed as:

$$G_M(s, r) = \sum_{i=1}^M \frac{\bar{P}_i \phi_i(r)}{s^2 + 2\xi_i \omega_i s + \omega_i^2} \quad (12)$$

where $M \ll N$. This truncation may cause error due to the removed modes which can be expressed as an error system model, $E(s, r)$:

$$\begin{aligned} E(s, r) &= G_N(s, r) - G_M(s, r) \\ &= \sum_{i=M+1}^N \frac{\bar{P}_i \phi_i(r)}{s^2 + 2\xi_i \omega_i s + \omega_i^2} \end{aligned} \quad (13)$$

In order to compensate the model truncation error, a correction term should be added to the truncated model (Halim, 2002b):

$$G_C(s, r) = G_M(s, r) + K(r) \quad (14)$$

where $G_C(s, r)$ and $K(r)$ are the corrected transfer function and correction term, respectively.

The correction term $K(r)$ involves the effects of removed modes of the system on the frequency range of interest, and can be expressed as:

$$K(r) = \sum_{i=M+1}^N \phi_i(r)k_i \quad (15)$$

where k_i is a constant term. The reasonable value of k_i should be determined by keeping the difference between $G_N(s, r)$ and $G_C(s, r)$ to be minimum, i.e. corrected system model should approach more to the higher ordered one given in equation (8). Moheimani (2000a) represents this condition by a cost function, J , which describes that the spatial H_2 norm of the difference between $G_N(s, r)$ and $G_C(s, r)$ should be minimized:

$$J = \ll W(s, r) \{G_N(s, r) - G_C(s, r)\} \gg_2^2 \quad (16)$$

The notation $\ll \dots \gg_2^2$ represents the spatial H_2 norm of a system where spatial norm definitions are given in (Moheimani, 2003). $W(s, r)$ is an ideal low-pass weighting function distributed spatially over the entire domain R with its cut-off frequency ω_c chosen to lie within the interval (ω_M, ω_{M+1}) (Moheimani, 2000a). That is:

$$|W(j\omega, r)| = \begin{cases} 1 & -\omega_c < \omega < \omega_{c+1}, r \in R \\ 0 & elsewhere \end{cases} \quad (17)$$

and $\omega_c \in (\omega_M, \omega_{M+1})$

where ω_M and ω_{M+1} are the natural frequencies associated with mode number M and $M + 1$, respectively. Halim (2002b) showed that, by taking the derivative of cost function J with respect to k_i and using the orthogonality of eigenfunctions, the general optimal value of the correction term, so called k_i^{opt} , for the spatial model of resonant systems, including the damping effect, can be shown to be:

$$k_i^{opt} = \frac{1}{4\omega_c\omega_i} \frac{1}{\sqrt{1-\xi_i^2}} \ln \left\{ \frac{\omega_c^2 + 2\omega_c\omega_i\sqrt{1-\xi_i^2} + \omega_i^2}{\omega_c^2 - 2\omega_c\omega_i\sqrt{1-\xi_i^2} + \omega_i^2} \right\} \bar{P}_i \quad (18)$$

An interesting result of equation (18) is that, if damping coefficient is selected as zero for each mode, i.e. undamped system, the resultant correction term is equivalent to those given

in references (Moheimani, 2000a, 2000c and 2000d) for an undamped system. Therefore, equation (18) can be represented as not only the optimal but also the general expression of the correction term.

So, following the necessary mathematical manipulations, one will obtain the corrected system model including the effect of out-of-range modes as:

$$G_C(s, r) = \sum_{i=1}^M \frac{\bar{P}_i \phi_i(r)}{s^2 + 2\xi_i \omega_i s + \omega_i^2} + \sum_{i=M+1}^N \phi_i(r) \left\{ \frac{1}{4\omega_c \omega_i} \frac{1}{\sqrt{1-\xi_i^2}} \ln \left\{ \frac{\omega_c^2 + 2\omega_c \omega_i \sqrt{1-\xi_i^2} + \omega_i^2}{\omega_c^2 - 2\omega_c \omega_i \sqrt{1-\xi_i^2} + \omega_i^2} \right\} \bar{P}_i \right\} \quad (19)$$

Consider the cantilevered smart beam depicted in Fig.1 with the structural properties given at Table 1. The beginning and end locations of the PZT patches $r_1 = 0.027m$ and $r_2 = 0.077m$ away from the fixed end, respectively. Note that, although the actual length of the passive beam is 507mm, the effective length, or span, reduces to 494mm due to the clamping in the fixture.

	Aluminum Beam	Passive	PZT
Length	$L_b = 0.494m$		$L_p = 0.05m$
Width	$w_b = 0.051m$		$w_p = 0.04m$
Thickness	$t_b = 0.002m$		$t_p = 0.0005m$
Density	$\rho_b = 2710kg/m^3$		$\rho_p = 7650kg/m^3$
Young's Modulus	$E_b = 69GPa$		$E_p = 64.52GPa$
Cross-sectional Area	$A_b = 1.02 \times 10^{-4} m^2$		$A_p = 0.2 \times 10^{-4} m^2$
Second Moment of Area	$I_b = 3.4 \times 10^{-11} m^4$		$I_p = 6.33 \times 10^{-11} m^4$
Piezoelectric charge constant	-		$d_{31} = -175 \times 10^{-12} m/V$

Table 1. Properties of the Smart Beam

The system model given in equation (8) includes N number of modes of the smart beam, where as N gets larger, the model becomes more accurate. In this study, first 50 flexural resonance modes are included into the model (i.e. $N=50$) and the resultant model is called *the full order model*:

$$G_{50}(s, r) = \sum_{i=1}^{50} \frac{\bar{P}_i \phi_i(r)}{s^2 + 2\xi_i \omega_i s + \omega_i^2} \quad (20)$$

However, the control design criterion of this study is to suppress only the first two flexural modes of the smart beam. Hence, the full order model is directly truncated to a lower order model, including only the first two flexural modes, and the resultant model is called *the truncated model*:

$$G_2(s, r) = \sum_{i=1}^2 \frac{\bar{P}_i \phi_i(r)}{s^2 + 2\xi_i \omega_i s + \omega_i^2} \quad (21)$$

As previously explained, the direct model truncation may cause the zeros of the system to perturb, which consequently affect the closed-loop performance and stability of the system considered (Clark, 1997). For this reason, the general correction term, given in equation (18), is added to the truncated model and the resultant model is called *the corrected model*:

$$G_C(s, r) = \sum_{i=1}^2 \frac{\bar{P}_i \phi_i(r)}{s^2 + 2\xi_i \omega_i s + \omega_i^2} + \sum_{i=3}^{50} \phi_i(r) \left\{ \frac{1}{4\omega_c \omega_i} \frac{1}{\sqrt{1-\xi_i^2}} \ln \left[\frac{\omega_c^2 + 2\omega_c \omega_i \sqrt{1-\xi_i^2} + \omega_i^2}{\omega_c^2 - 2\omega_c \omega_i \sqrt{1-\xi_i^2} + \omega_i^2} \right] \bar{P}_i \right\} \quad (22)$$

where the cut-off frequency, based on the selection criteria given in equation (17), is taken as:

$$\omega_c = (\omega_2 + \omega_3) / 2 \quad (23)$$

The assumed-modes method gives the first three resonant frequencies of the smart beam as shown in Table 2. Hence, the cut-off frequency becomes 79.539 Hz. The performance of model correction for various system models obtained from different measurement points along the beam is shown in Fig.3 and Fig.4.

Resonant Frequencies	Value (Hz)
ω_1	6.680
ω_2	41.865
ω_3	117.214

Table 2. First three resonant frequencies of the smart beam

The error between full order model-truncated model, and the error between full order model-corrected model, so called the error system models \bar{E}_{F-T} and \bar{E}_{F-C} , allow one to see the effect of model correction more comprehensively.

$$\bar{E}_{F-T} = G_N(s, r) - G_M(s, r) \quad (24)$$

$$\bar{E}_{F-C} = G_N(s, r) - G_C(s, r) \quad (25)$$

The frequency responses of the error system models are shown in Fig.5 and Fig.6. One can easily notice from the aforementioned figures that, the error between the full order and corrected models is less than the error between the full order and truncated ones in a wide range of the interested frequency bandwidth. That is, the model correction minimizes error considerably and makes the truncated model approach close to the full order one. The error between the full order and corrected models is smaller at low frequencies and around 50 Hz it reaches a minimum value. As a result, model correction reduces the overall error due to model truncation, as desired.

In this study, the experimental system models based on displacement measurements were obtained by nonparametric identification. The smart beam was excited by piezoelectric patches with sinusoidal chirp signal of amplitude 5V within bandwidth of 0.1-60 Hz, which covers the first two flexural modes of the smart beam. The response of the smart beam was acquired via laser displacement sensor from specified measurement points. Since the patches are relatively thin compared to the passive aluminum beam, the system was considered as 1-D single input multi output system, where all the vibration modes are flexural modes. The open loop experimental setup is shown in Fig.7.

In order to have more accurate information about spatial characteristics of the smart beam, 17 different measurement points, shown in Fig.8, were specified. They are defined at 0.03m intervals from tip to the root of the smart beam.

The smart beam was actuated by applying voltage to the piezoelectric patches and the transverse displacements were measured at those locations. Since the smart beam is a spatially distributed system, that analysis resulted in 17 different single input single output system models where all the models were supposed to share the same poles. That kind of

analysis yields to determine uncertainty of resonance frequencies due to experimental approach. Besides, comparison of the analytical and experimental system models obtained for each measurement points was used to determine modal damping ratios and the uncertainties on them. That is the reason why measurement from multiple locations was employed. The rest of this section presents the comparison of the analytical and experimental system models to determine modal damping ratios and clarify the uncertainties on natural frequencies and modal damping ratios.

Consider the experimental frequency response of the smart beam at point $r = 0.99L_b$. Because experimental frequency analysis is based upon the exact dynamics of the smart beam, the values of the resonance frequencies determined from experimental identification were treated as being more accurate than the ones obtained analytically, where the analytical values are presented in Table 2. The first two resonance frequencies were extracted as 6.728 Hz and 41.433 Hz from experimental system model. Since the analytical and experimental models should share the same resonance frequencies in order to coincide in the frequency domain, the analytical model for the location $r = 0.99L_b$ was coerced to have the same resonance frequencies given above. Notice that, the corresponding measurement point can be selected from any of the measurement locations shown in Fig.8. Also note that, the analytical system model is the corrected model of the form given in equation (22). The resultant frequency responses are shown in Fig.9.

The analytical frequency response was obtained by considering the system as undamped. The point $r = 0.99L_b$ was selected as measurement point because of the fact that the free end displacement is significant enough for the laser displacement sensor measurements to be more reliable. After obtaining both experimental and analytical system models, the modal damping ratios were tuned until the magnitude of both frequency responses coincide at resonance frequencies, i.e.:

$$\left| G_E(s, r) - G_C(s, r) \right|_{\omega=\omega_i} < \lambda \quad (26)$$

where $G_E(s, r)$ is the experimental transfer function and λ is a very small constant term. Similar approach can be employed by minimizing the 2-norm of the differences of the displacements by using least square estimates (Reinelt, 2002).

Fig.10 shows the effect of tuning modal damping ratios on matching both system models in frequency domain where λ is taken as 10^{-6} . Note that each modal damping ratio can be tuned independently.

Consequently, the first two modal damping ratios were obtained as 0.0284 and 0.008, respectively. As the resonance frequencies and damping ratios are independent of the location of the measurement point, they were used to obtain the analytical system models of the smart beam for all measurement points. Afterwards, experimental system identification was again performed for each point and both system models were again compared in

frequency domain. The experimentally identified flexural resonance frequencies and modal damping ratios were determined by tuning for each point and finally a set of resonance frequencies and modal damping ratios were obtained. The amount of uncertainty on resonance frequencies and modal damping ratios can also be determined by spatial system identification. There are different methods which can be applied to determine the uncertainty and improve the values of the parameters ω and ξ such as boot-strapping (Reinelt, 2002). However, in this study the uncertainty is considered as the standard deviation of the parameters and the mean values are accepted as the final values, which are presented at Table 3.

	ω_1 (Hz)	ω_2 (Hz)	ξ_1	ξ_2
Mean	6.742	41.308	0.027	0.008
Standard Deviation	0.010	0.166	0.002	0.001

Table 3. Mean and standard deviation of the first two resonance frequencies and modal damping ratios

For more details about spatial system identification one may refer to (Kırçalı, 2006a). The estimated and analytical first two mode shapes of the smart beam are given in Fig.11 and Fig.12, respectively (Kırçalı, 2006a).

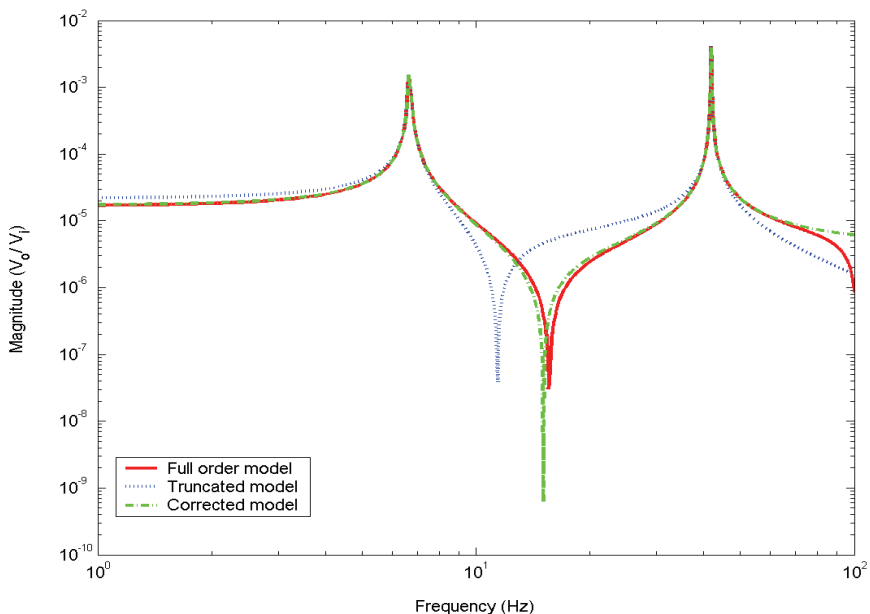


Fig. 3. Frequency response of the smart beam at $r = 0.14L_b$

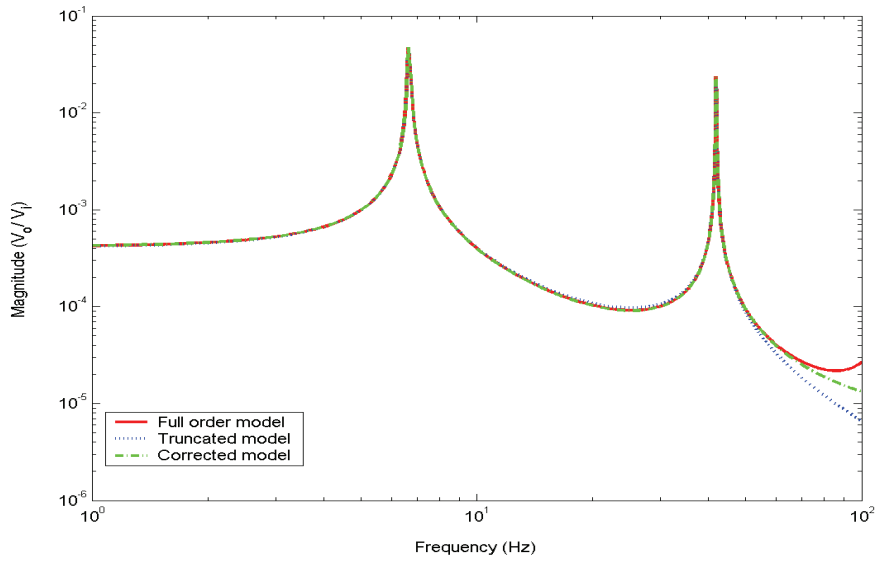


Fig. 4. Frequency response of the smart beam at $r = 0.99L_b$

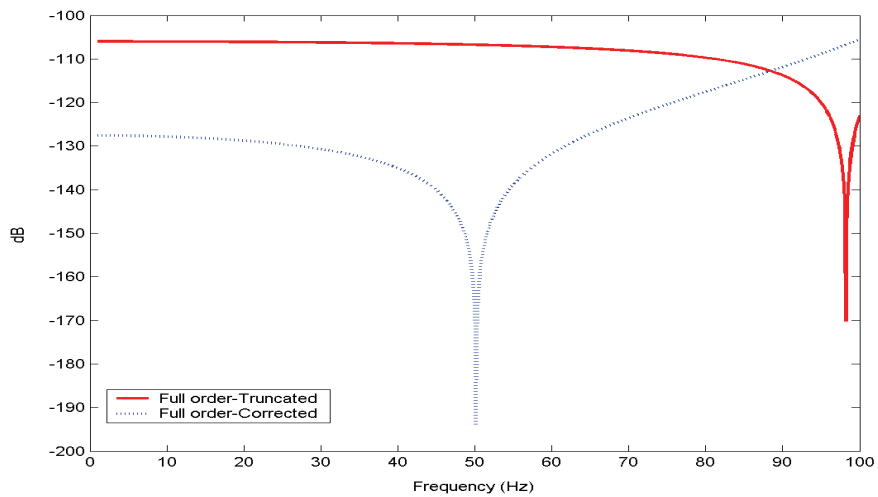


Fig. 5. Frequency responses of the error system models at $r = 0.14L_b$

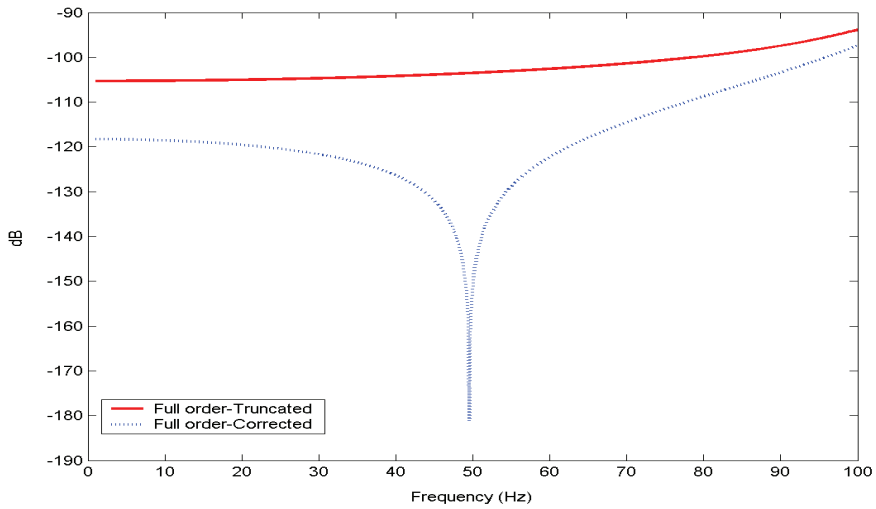


Fig. 6. Frequency responses of the error system models at $r = 0.99L_b$

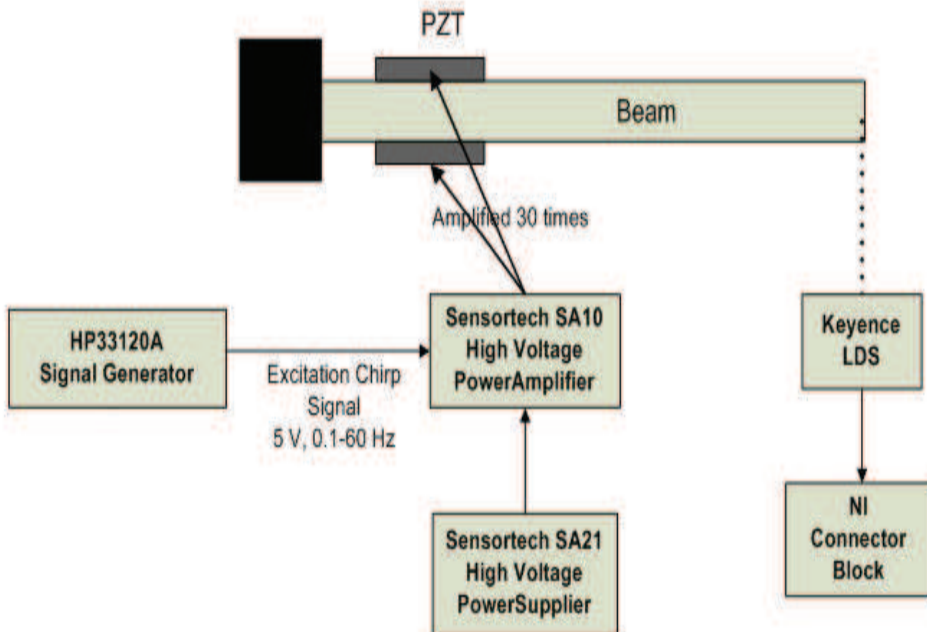


Fig. 7. Experimental setup for the spatial system identification of the smart beam

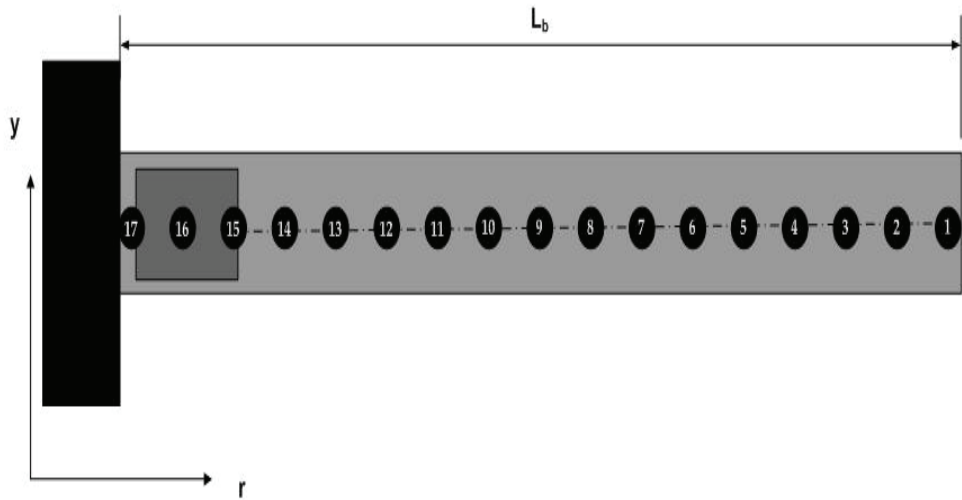


Fig. 8. The locations of the measurement points

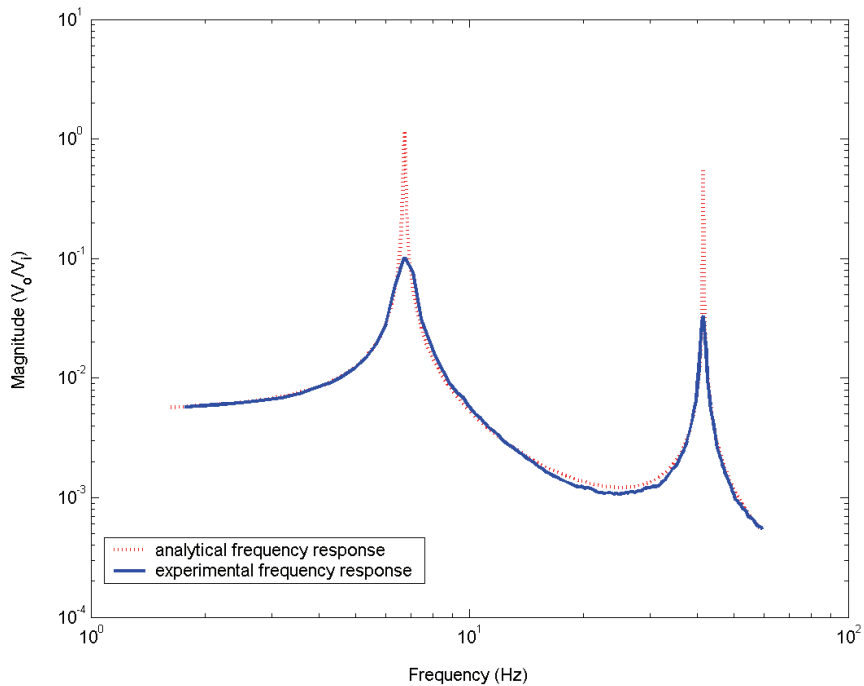


Fig. 9. Analytical and experimental frequency responses of the smart beam at $r=0.99 L_b$

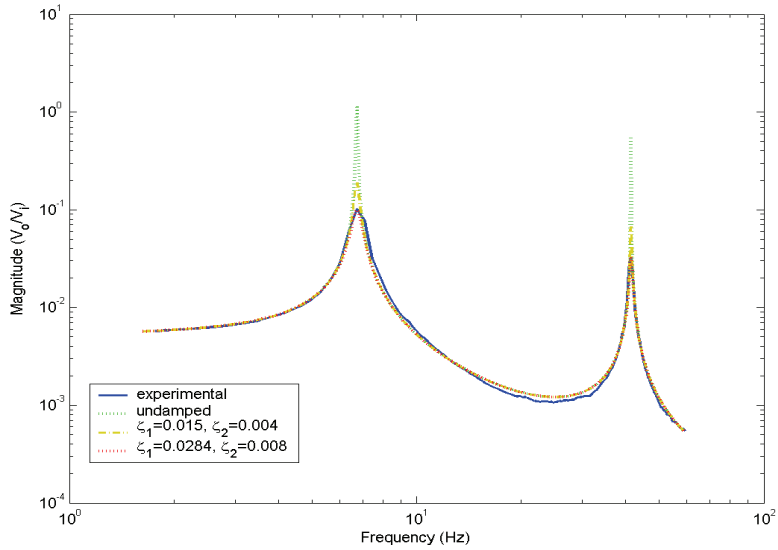


Fig. 10. Experimental and tuned analytical frequency responses at $r=0.99 L_b$

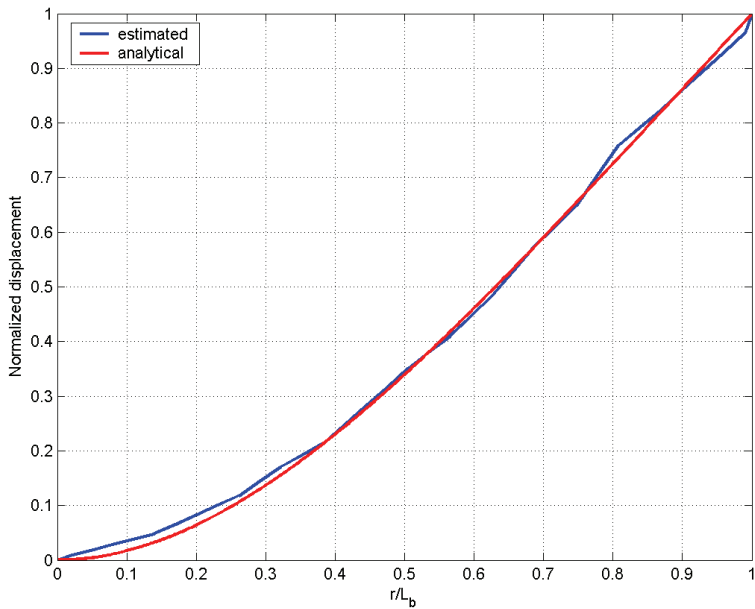


Fig. 11. First mode shape of the smart beam

Thank You for previewing this eBook

You can read the full version of this eBook in different formats:

- HTML (Free /Available to everyone)
- PDF / TXT (Available to V.I.P. members. Free Standard members can access up to 5 PDF/TXT eBooks per month each month)
- Epub & Mobipocket (Exclusive to V.I.P. members)

To download this full book, simply select the format you desire below

